ACTN4 regulates the stability of RIPK1 in melanoma

Yuan Yuan Zhang,[1] Hessam Tabataba,[2] Xiao Ying Liu,[1,3] Jia Yu Wang, [2] Xu Guang Yan,[2] Margaret Farrelly,[2] Chen Chen Jiang,[1,4] Su Tang Guo,[2,5] Tao Liu,[6] Hung-Ying Kao,[7] Rick F. Thorne,[8] Xu Dong Zhang,[2,4,*] Lei Jin[1,4,*]

[1]School of Medicine and Public Health, The University of Newcastle, NSW, 2308, Australia

[2]School of Biomedical Sciences and Pharmacy, The University of Newcastle, NSW, 2308, Australia

[3]School of Life Science, Anhui Medical University, Anhui, 230000, China

[4]Cancer Research Program, Hunter Medical Research Institute, NSW, 2305, Australia

[5]Department of Molecular Biology, Shanxi Cancer Hospital and Institute, Shanxi, 030013, China

[6]Children's Cancer Institute Australia for Medical Research, University of New South Wales, Sydney, NSW 2750, Australia

[7]Department of Biochemistry, Case Western Reserve University, Cleveland, Ohio 44106, United States

[8]School of Environmental and Life Sciences, University of Newcastle, NSW 2308, Australia.

*Correspondence: Lei Jin or Xu Dong Zhang, LS3-49, Life Science Building, University of Newcastle, Callaghan, NSW, Australia. Ph: 61 2 49218906. Fax: 61 2 49217311.

Email: Lei.Jin@newcastle.edu.au or Xu.Zhang@newcastle.edu.au

Running title: ACTN4 regulates RIPK1 in melanoma

Key Words: ACTN4, RIPK1, cell proliferation, Melanoma

ABSTRACT

The actin crosslinking protein α-actinin-4 (ACTN4) is emerging as an important contributor to the pathogenesis of cancer. This has largely been attributed to its role in regulating cytoskeleton organization and its involvement in transcriptional regulation of gene expression. Here we report a novel function of ACTN4 as a scaffold necessary for stabilization of receptor-interacting protein kinase 1 (RIPK1) that we have recently found to be an oncogenic driver in melanoma. ACTN4 bound to RIPK1 and cellular inhibitor of apoptosis protein 1 (cIAP1) with its actin-binding domain at the N-terminus and the CaM-like domain at the C-terminus, respectively. This facilitated the physical association between RIPK1 and cIAP1 and was critical for stabilization of RIPK1 that in turn activated NF-κB. Functional investigations showed that silencing of ACTN4 suppressed melanoma cell proliferation and retarded melanoma xenograft growth. In contrast, overexpression of ACTN4 promoted melanocyte and melanoma cell proliferation and moreover, prompted melanocyte anchorage-independent growth. Of note, the expression of ACTN4 was transcriptionally activated by NF-κB. Taken together, our findings identify ACTN4 as an oncogenic regulator through driving a feedforward signalling axis of ACTN4-RIPK1-NF-κB, with potential implications for targeting ACTN4 in the treatment of melanoma.

INTRODUCTION

Alpha-actinin-4 (ACTN4) is a member of the α-actinin family of filamentous actin crosslinking proteins important for regulation of cytoskeletal integrity and cell movement [1, 2, 3]. Like other family members, ACTN4 contains an N-terminal actin-binding region with two calponin-homology repeats, a central rod domain with 4 spectrin-like repeats (SR) that is essential for anti-parallel dimerization of ACTN4, and a calmodulin (CaM)-like domain at the C-terminus [1, 4, 5]. Although ACTN4 is ubiquitously expressed in normal non-muscle cells [1, 6], its expression is frequently increased in various types of cancer cells including melanoma cells and high ACTN4 expression levels are often correlated with disease progression and poor patient prognosis [7, 8, 9].

Indeed, there is increasing evidence pointing to a role of ACTN4 in the pathogenesis of cancer [7, 9, 10, 11, 12]. This is not only due to its critical involvement in regulation of cancer cell adhesion, invasion, and metastasis [3, 13, 14], but also closely associated with its role in regulation of signalling pathways through its interaction with a large array of proteins [15, 16, 17]. For example, ACTN4 targets the p65/RelA subunit of NF-κB to the nucleus in breast cancer cells upon stimulation with tumour necrosis factor α (TNF-α) or epithelial growth factor (EGF), where it functions as a co-factor for transactivation of NF-κB target genes [15, 18]. Moreover, ACTN4 interacts with Akt1 and promotes its phosphorylation (activation) thus leading to enhanced cell survival and proliferation [19]. Although the activity of ACTN4 is known to be modulated by multiple mechanisms such as processing by calpain protease, phosphorylation by protein kinases, and binding to phosphatidylinositol intermediates [20, 21, 22], how ACTN4 expression is regulated remains to be defined.

Receptor-interacting protein kinase 1 (RIPK1) is a Ser/Thr protein kinase that plays an important role in cell survival and death signal transduction and is a critical determinant of cell fate in response to cellular stress [23, 24, 25, 26, 27, 28], in particular, in response to activation of death receptors such as TNF receptor 1 (TNFR1). Upon TNFR1 stimulation, prosurvival complex I is formed via recruiting RIPK1 and other proteins involving cIAP1, cIAP2, TRADD, and TRAF2. [24, 29]. This results in

stabilization of RIPK1 through K63-linked polyubiquitination by cIAPs [26, 30]. K63-linked polyubiquitin chains serve as substrates for binding of the TAB2/TAB3/TAK1 complex and NEMO, leading to activation of NF-κB [26, 29, 31]. When cIAPs are blocked, RIPK1 is deubiquitinated and its function is switched to that of promoting apoptosis, or alternatively, necroptosis in certain types of cells [24, 32].

RIPK1 is often upregulated and promotes cell proliferation via activation of NF-κB in melanoma [26]. Stabilization of RIPK1 by cIAPs is critical for its increased expression [26, 30]. Here we demonstrate that ACTN4 is necessary for cIAP-mediated stabilization of RIPK1 through acting as a scaffold to enable the physical association between cIAP1 and RIPK1, and thus plays a critical role in activation of NF-κB and promotion of melanoma cell proliferation. Moreover, we show that NF-κB signalling is responsible for ACTN4 transcriptional upregulation in melanoma cells.

RESULTS

ACTN4 promotes melanoma cell proliferation and melanoma xenograft growth

To examine the functional significance of ACTN4, we silenced ACTN4 in Mel-JD and Mel-CV, two melanoma cell lines that expressed relatively high levels of ACTN4 among a panel of melanoma cell lines (Supplementary Fig. S1a), by shRNA knockdown (Fig. 1a). ACTN4 silencing inhibited cell migration and invasion (Supplementary Fig. S1b and c), consistent with its well-established role as an actin-crosslinking protein [1, 14]. Strikingly, it also attenuated BrdU incorporation and clonogenicity in Mel-JD and Mel-CV cells (Fig. 1b and c), suggesting that ACTN4 plays a part in regulating melanoma cell proliferation. In support, overexpression of ACTN4 in IgR3 and Mel-RM cells that expressed relatively low levels of endogenous ACTN4 promoted melanoma cell proliferation (Fig. 1d-f, Supplementary Fig. S1a). Moreover, overexpression of ACTN4 in melanocytes similarly enhanced cell proliferation and resulted in anchorage-independent growth (Fig. 1g-i).

To determine whether ACTN4 affects melanoma growth *in vivo*, we transplanted Mel-CV cells with or without ACTN4 stably silenced by shRNA subcutaneously into nu/nu mice (Fig. 1j). Suppression of ACTN4 retarded growth of Mel-CV xenografts (Fig. 1k and l). This was associated with reduced expression of Ki67 (Fig. 1m). Collectively, these results highlight the contribution of ACTN4 to the pathogenesis of melanoma through promoting cell proliferation apart from its role in cell invasion and metastasis.

ACTN4 promotes melanoma cell proliferation through NF-κB independently of its nuclear translocation

Since NF-κB is constitutively activated and plays an important role in promoting cell proliferation in melanoma cells, we examined whether ACTN4-mediated melanoma cell proliferation is associated with NF-κB activation. ACTN4 silencing in Mel-CV and Mel-JD cells reduced, whereas overexpression of ACTN4 in IgR3 and Mel-RM cells enhanced, NF-κB activity (Fig. 2a and b). Consistently, silencing of ACTN4 in Mel-CV and Mel-JD cells resulted in increased IκBα levels with

an accompanying decrease in serine 32/36 phosphorylation (p-IκBα S32/36), which is known to direct the degradation of IκBα (Fig. 2c). Conversely, overexpression of ACTN4 in IgR3 and Mel-RM cells resulted in increased S32/36 phosphorylation and decreased IκBα levels (Fig. 2d). The functional significance of NF-κB in ACTN4-mediated melanoma cell proliferation was demonstrated by introduction of a non-degradable mutant of IκBα (IκBα-S32AS36A), which inhibited IgR3 and Mel-RM cell proliferation even when ACTN4 was overexpressed (Fig. 2e and f). Moreover, the NF-κB inhibitors PS1145 and BAY-11-7082 abolished the enhanced proliferation in IgR3 and Mel-RM cells triggered by ACTN4 overexpression (Fig. 2g). These results indicate that NF-κB activation is critical for ACTN4-mediated melanoma cell proliferation. In support, silencing of IκBα that caused NF-κB hyperactivation was sufficient to override completely the anti-proliferative effect of ACTN4 silencing (Fig. 2h and i) [26, 33].

Intriguingly, ACTN4 was exclusively located to the cytoplasm in Mel-CV and Mel-JD cells (Fig. 2j and k). This suggests that ACTN4-mediated NF-κB activation in these cells is not associated with its relocation into the nucleus [15, 18]. Indeed, while the p65 subunit of NF-κB was increased in the nucleus, relocation of ACTN4 was not observed in melanoma cells exposed to TNFα (Fig. 2j and k), in contrast to the movement of ACTN4 along with p65 into the nucleus in MCF-7 cells in response to TNFα (Fig. 2k) [15, 16]. Thus, ACTN4 promotes NF-κB activation independently of its relocation to the nucleus in a cell type-dependent manner [15, 16].

ACTN4 promotes NF-κB activation through RIPK1 in melanoma

To define the mechanism by which ACTN4 promotes NF-κB independently of its translocation into the nucleus, we carried out mass spectrometry analysis of immunoprecipitates generated with an anti-ACTN4 antibody in total protein extracts of Mel-CV cells. One of the proteins co-precipitated with ACTN4 was identified as RIPK1 (Supplementary Fig. S2a). This association was confirmed by reciprocal co-precipitation using an antibody against RIPK1 or ACTN4 (Fig. 3a and b). Of note, no physical association was observed between RIPK1 and another α-actinin family member ACTN1 (Supplementary Fig. S2b). Moreover, GST-tagged ACTN4 pulled down myc-tagged RIPK1 from

whole cell lysates of IgR3 cells bearing exogenous myc-fused RIPK1 (Fig. 3c), consolidating that ACTN4 and RIPK1 are bona fide binding partners.

To determine whether RIPK1 was mechanistically involved in ACTN4-mediated activation of NF-κB, we silenced RIPK1 in IgR3 and Mel-RM cells overexpressing ACTN4 (Fig. 3d). Examination of NF-κB activity showed that reduction in RIPK1 abolished the increase in NF-κB activation caused by ACTN4 overexpression (Fig. 3e). Moreover, RIPK1 silencing inhibited ACTN4 overexpression-triggered promotion of cell proliferation (Fig. 3f). In contrast, induction of RIPK1 in MM200 cells carrying an inducible RIPK1-expressing system in response to doxycycline abolished ACTN4 knockdown-triggered inhibition of NF-κB activation and cell proliferation (Fig. 3g-i) [26]. Together, these results indicate that RIPK1 is necessary for activation of NF-κB and promotion of proliferation by ACTN4.

ACTN4 is critical for stabilization of RIPK1 in melanoma

ACTN4 silencing downregulated RIPK1, but did not affect the expression of cIAP1, which is the major cIAP that polyubiquitinizes RIPK1 at K63 leading to its stabilization [26, 30, 34], in Mel-CV and Mel-JD cells (Fig. 4a). On the other hand, overexpression of ACTN4 in IgR3 and Mel-RM resulted in upregulation of RIPK1 (Fig. 4b). These changes in RIPK1 expression were not associated with alterations in its mRNA levels (Fig. 4c and d), suggesting that they resulted through posttranscripional regulation. Indeed, treatment with the proteasome inhibitor MG132 abolished downregulation of RIPK1 caused by ACTN4 silencing (Fig. 4e). Moreover, ACTN4 silencing shortened half-life time of RIPK1 (Fig. 4f), triggered reduction in K63-linked RIPK1 polyubiquitination and reduced the association between RIPK1 and cIAP1 (Fig. 4g and h). Of note, the levels of ACTN4 and RIPK1 expression were positively correlated in melanoma cell lines (Supplementary Fig. S1a). Therefore, ACTN4 is necessary for stabilization of RIPK1.

We mapped the functional domain(s) of RIPK1 required for its interaction with ACTN4 using domain deletion mutants of RIPK1. Flag-tagged RIPK1 constructs lacking the kinase domain (KD),

intermediate domain (ID), or death domain (DD) (Flag-RIPK1-ΔKD, Flag- RIPK1-ΔID and Flag-RIPK1-ΔDD, respectively; Fig. 5a) were introduced into IgR3 cells along with HA-tagged ACTN4 (HA-ACTN4). HA-ACTN4 was readily co-precipitated with Flag-RIPK1-ΔDD but not Flag-RIPK1-ΔKD or Flag- RIPK1-ΔID (Fig. 5b), indicating that both the KD and ID of RIPK1 are necessary for its interaction with ACTN4. In support, Flag-RIPK1-ΔDD but not Flag-RIPK1-ΔKD and Flag-RIPK1-ΔID were pulled down by GST-ACTN4 (Fig. 5c). Of note, although RIPK1 KD was necessary for its association with ACTN4, the kinase activity of RIPK1 was not involved, in that treatment with necrostatin-1, a specific inhibitor of RIPK1 kinase activity, did not impinge on the interaction between ACTN4 and RIPK1 (Fig. 5d).

A similar approach was used to investigate the functional domain(s) of ACTN4 required for binding to RIPK1. Constructs of Flag-tagged ACTN4 with the actin-binding domain (ABD), the rod domain (RD), or the CaM-like domain (CLD) deleted (Flag-ACTN4-ΔABD, Flag-ACTN4-ΔRD, and Flag-ACTN4-ΔCLD, respectively; Fig. 5e) were co-introduced into IgR3 cells along with myc-tagged RIPK1 (Myc-RIPK1). Both Flag-ACTN4-ΔRD and Flag-ACTN4-ΔCLD, but not ACTN4-ΔABD, were co-precipitated with RIPK1, suggesting that ACTN4 binds to RIPK1 through its ABD (Fig. 5f).

Similar to RIPK1, cAIP1 also appeared to be a binding partner of ACTN4, as cIAP1 and ACTN4 were co-precipitated in Mel-CV cells (Fig. 5g). Moreover, GST-ACTN4 pulled down endogenous cIAP1 purified from IgR3 cells (Fig. 5h). In contrast to binding of RIPK1 to ACTN4 at its ABD, cIAP1 was co-precipitated with Flag-ACTN4-ΔABD and Flag-ACTN4-ΔRD, but not Flag-ACTN4-ΔCLD (Fig. 5i), indicating that it binds to the CLD at the C-terminus of ACTN4.

NF-κB transcriptionally activates ACTN4 in melanoma

Having demonstrated the mechanism by which ACTN4 promotes NF-κB activation and cell proliferation, we focused on investigating how ACTN4 is regulated. The expression of ACTN4 mRNA was commonly elevated in a panel of melanoma cell lines compared to a melanocyte line (Fig. 6a), which was not due to its gene amplification, as qPCR analysis of genomic DNA showed that

genomic alterations of the *ACTN4* gene were rare in the cell lines (Supplementary Fig. S3). In support, analysis of TCGA datasets did not show any significant *ACTN4* gene copy number variations in melanomas (www.cbioportal.org) [35, 36]. The turnover rate of ACTN4 mRNA in melanoma cells with relatively high or low expression levels appeared similar to that in melanocytes as shown in actinomycin D-chasing assays (Fig. 6b), indicating that its increase in melanoma cells was due to transcriptional upregulation rather than changes in its stability [26, 37].

Through bioinformatics analysis, we identified a fragment (-984/-672; numbers relative to the transcription start site) at the core promoter region of the *ACTN4* gene that contained 3 consensus binding sites for NF-κB (Fig. 6c). To test whether this fragment is transcriptionally active in response to NF-κB, we introduced pGL3 basic-based luciferase reporter constructs containing the -1115/+251 region with or without the -984/-672 fragment deleted into Mel-CV and Mel-JD cells (Fig. 6d). While pGL3-ACTN4 (-1115/+251) was transcriptionally active, deletion of the -984/-672 fragment abolished the transcriptional activity (Fig. 6e). Similarly, treatment with the NF-κB inhibitor PS1145 or BAY-11-7082 diminished the transcriptional activity of pGL3-ACTN4 (-1115/+251) (Fig. 6f). In contrast, co-introduction of IκBα siRNA led to increases in the activity of pGL3-ACTN4 (-1115/+251) with the intact -984/-672 fragment, but not in the construct with the fragment deleted (Fig. 6g and h). These results indicate that NF-κB activity is required for transcriptional activation of the *ACTN4* promoter. Indeed, the p65 subunit of NF-κB was physically associated with the -984/-672 fragment of the promoter as shown in ChIP assays (Fig. 6i).

DISCUSSION

As an actin-cross-linking protein, the role of ACTN4 in cytoskeleton organization and cell adhesion and movement has been well-documented [1, 3]. In many types of cancers, ACTN4 expression is upregulated with its function characteristically manifested by promotion of cancer cell invasion and metastasis [1, 14]. Nevertheless, there has been increasing evidence showing the involvement of ACTN4 in regulating cell proliferation through modulation of gene transcription and signal transduction [1, 15, 16]. In particular, ACTN4 promotes activation of NF-κB in a number types of cancer cells [1, 15]. This has been primarily ascribed to its co-translocation with the p65 subunit of NF-κB from the cytoplasm to the nucleus, where it functions as a transcriptional coactivator in at least some type of cells such as breast cancer cells and A431 epidermoid carcinoma cells [1, 38]. However, we found in this study that ACTN4 promoted NF-κB activation independently of its nuclear localization in melanoma cells, suggesting that ACTN4 is able to mediate activation of NF-κB in varying cellular compartments in a cell type-dependent manner.

ACTN4 is predominantly located to the cytoplasm in the majority types of cells [15]. Nevertheless, the interaction of its rod domain with proteins of the nuclear pore enables it to shuttle across the nuclear pore complexes [39]. Although the signal(s) that drives ACTN4 to commute between the nucleus and cytoplasm remains to be fully uncovered, stimulation of breast cancer cells with EGF or TNFα results in nuclear relocation of ACTN4 from the cytoplasm in complex with p65 [15, 18]. Of note, while ACTN4 has also been found to be entirely located to the nucleus in some types of cells [3], we found that ACTN4 was exclusively located to the cytoplasm in melanoma cells even upon stimulation with TNFα. This distinct localization of ACTN4 was unlikely due to mutations in its gene, as exon-sequencing did not identify any mutations in the melanoma cell lines included in this study (not shown). Given the large number of binding partners of ACTN4 [16, 18, 19], one possibility is that ACTN4 may only be a "passenger" rather than an "autonomous vehicle" when shuttling across the nuclear member. In support, our results indicated that ACTN4 silencing did not affect nuclear localization of p65 in melanoma cells. Consistently, silencing of ACTN4 did not disrupt

translocation of p65 from the cytoplasm to the nucleus in response to TNFα in MCF7 breast cancer cells [1, 15]. p65 contains a classic nuclear localization signal (NLS) that can bind to importin α3, thus enabling its nuclear localization [40].

An important finding of this study is that promotion of NF-κB activation by ACTN4 is mediated by RIPK1, which we have recently shown to be critical for activation of NF-κB in melanoma cells under steady-state conditions and upon stimulation with TNFα [26]. The role of RIPK1 was primarily demonstrated by the findings that RIPK1 silencing diminished ACTN4 overexpression-induced increases in NF-κB activation, whereas RIPK1 overexpression abolished inhibition of NF-κB activation caused by ACTN4 knockdown. Moreover, ACTN4 was physically associated with RIPK1 and was critical for RIPK1 expression through promoting its stabilization. K63-linked polyubiquitination of RIPK1 by cIAPs, in particular, cIAP1, is essential for RIPK1 stabilization and subsequent activation of NF-κB [26, 30]. Indeed, we found that cIAP1 also bound to ACTN4 in melanoma cells. Collectively, these results identify RIPK1 and cIAP1 as two novel binding partners of ACTN4 and indicate that ACTN4 forms a ternary structure with cIAP1 and RIPK1 that is important for activation of NF-κB in melanoma cells.

Although the SR repeats at the rod domain of ACTN4 is well known to serve as a protein-protein interaction platform for binding of ACTN4 with its partners [6], the rod domain appeared dispensable for the association between ACTN4 and RIPK1 and cIAP1 in melanoma cells. Instead, RIPK1 bound to the ABD of ACTN4 at its N-terminus, whereas cIAP1 was associated with the CLD at the C-terminus of ACTN4. Considering that approximately 70% of ACTN4 molecules form dumbbell-like anti-parallel homodimers through the rod domain thus enabling the ABD head of one molecule to be in close proximity to the CLD of a neighboring molecule [1, 41], we proposed a model where dimerization of ACTN4 in an anti-parallel fashion is important for bringing RIPK1 and cIAP1 to proximity, thus enabling their physical association (Supplementary Fig. S4).

ACTN4 was found to be transcriptionally upregulated by NF-κB. This, along with the findings that ACTN4 was critical for stabilization of RIPK1 that in turn played an important role in activation of NF-κB suggest that a feedforward signal axis of NF-κB-ACTN4-RIPK1 is operating to maintain high levels of de novo NF-κB activation in melanoma cells. This is of particular interest in that we have previously uncovered the existence of a NF-κB-cIAP1-RIPK1 feedforward signal pathway that is necessary for activation of NF-κB [26]. Since both cIAP1 and ACTN4 are transcriptional targets of NF-κB, it seems that these pathways are two integrated loops of the same feedforward signal network (Supplementary Fig. S4) [26, 42]. As reported previously, autocrine TNFα is an essential built-in apparatus and an extracellular driver of the network, as it is also transcriptionally upregulated by NF-κB and stimulates the recruitment of RIPK1 to complex I where it is polyubiquitinated at K63 by cIAPs leading to activation of NF-κB (Supplementary Fig. S4) [26].

A practical implication of this study is the potential application of ACTN4 inhibition in the treatment of melanoma. Silencing of ACTN4 not only inhibited melanoma cell proliferation, but also retarded melanoma xenograft growth *in vivo*. However, whether targeting ACTN4 directly *in vivo* is feasible needs to be further investigated.

MATERIALS AND METHODS

Cell lines and human tissues

Melanoma cells were cultured using DMEM plus 5% FCS [43]. Human melanocytes HEMn-MP were obtained from Banksia Scientific (Bulimba, QLD, Australia) which were maintained in 254 medium with human melanocyte growth supplement (HMGS) [37]. Cells were regularly tested for mycoplasma contamination and the Applied Biosystems AmpFISTR Identifiler PCR Amplification Kit (Mulgrave, VIC, Australia) together with GeneMarker V1.91 software (SoftGenetics LLC, State College, PA) were used to confirm the authenticity of each cell line. From the panel of 16 markers tested, each cell line had a distinct profile [44]. Approval was obtained from the University of Newcastle Human Research Ethics Committee for the studies using human tissues.

Antibodies and reagents

Antibodies against ACTN4, ACTN1, RIPK1 (IP), cIAP1, p65, GST, Lamin A/C and GAPDH were obtained from Santa Cruz Biotechnology (Santa Cruz, CA). The RIPK1 antibody from BD Biosciences was used for Western blotting (Marrickville, NSW, Australia). Phospho-IκBα, IκBα, Ki-67, HA-tag, Myc-tag and β-tubulin antibodies were purchased from Cell Signaling Technology (Beverly, MA). The antibody against K63-linked ubiquitin was supplied by Novus Biologicals (Littleton, CO). The Flag antibody was from Sigma-Aldrich (Castle Hill, NSW, Australia). The TrueBlot® secondary antibodies used in immunoprecipitation were from Rockland Immunochemicals (Limerick, PA). The RIPK1 kinase inhibitor known as Necrostatin-1 (Nec-1) was from Selleckchem (Houston, TX). TNF-α, Doxycycline, MG132, Actinomycin D, the NF-κB inhibitors BAY-11-7082 and PS1145were purchased from Sigma-Aldrich (Castle Hill, NSW, Australia). Cycloheximide was from MP Biomedicals (Seven Hills, NSW). The kit used for the NF-κB reporter assay was sourced from QIAGEN (Valencia, CA). A list of antibodies and reagents were shown in Supplementary Table S1 and S2.

Immunofluorescence (IF) staining

Fixation of cells was carried out using paraformaldehyde (4%), protected from light for 15 mins at room temperature. Slides were rinsed in PBS for three times (5 mins each), then permeabilised for 5 mins in 0.2% TX-100. Slides were kept in blocking buffer for 60 mins and then washed in PBS for 5 mins before being incubated with the primary antibody (ACTN4) at 4°C overnight. Secondary antibody against mouse was labelled with Alexa Fluor 488. Samples were observed under a fluorescence microscope (Zeiss).

Immunohistochemistry (IHC)

The procedure for IHC staining and quantitation has been described in previous publications [45]. Tissue was fixed in 10% buffered formalin. Antigen retrieval was achieved by placing slides with tissue into a pressure cooker at 125°C for 30 seconds. The tissue was stained using a Dako Envision HRP Detection system/DAB according to the manufacturer's protocol.

Clonogenic assays

Cells were seeded in6-well plates at 2000 cells/well and were treated with the indicated reagents 24 hours later. After 1-2 weeks until cells in control plates had formed colonies, cells were rinsed with PBS, subjected to 10 mins of methanol fixation on ice, then stained with crystal violet (0.5%). The crystal violet was carefully rinsed off with tap water and plates were air-dried at room temperature.

Cell proliferation assays

Proliferation assays were carried out with the BrdU Cell Proliferation Assay kit obtained from Cell Signaling Technology. Concisely, cells were seeded into 96-well plates at 5000 cells/well and treated with the indicated reagents 24 hours later. 10 μl of 10×BrdU solution was added in 100 μl medium per well followed by 4 hours incubation in incubator. The incorporated BrdU was detected by the BrdU mouse mAb after cells fixation and DNA denaturation. The absorbance was read by a Synergy™ 2 microplate reader (BioTek, VT) at 450nm.

NF-κB reporter assays and Luciferase assays

NF-κB activity assays were carried out using a Qiagen assay kit [46]. Briefly, cells were seeded to reach 90% confluency in a 96-well plate at the time of transfection. The NF-κB activity reporter was transfected into the cells with or without co-transfection with the indicated cDNAs or siRNAs followed by the desired treatment. The Dual-Luciferase Reporter Assay (Promega) procedure has been previously described [43].

Anchorage-independent cell growth

5 x 10^4 cells were cultured in 12-well culture plates using a two-layer agar system (0.3% agar plating layer on top of 0.6% base agar layer). Cells were incubated at 37°C in humidified incubator for a further 30 days feeding with cell culture medium twice a week. Cell colonies were counted using a light microscope.

Western blotting and Immunoprecipitation (IP)

Procedures for Western blotting and IP have been described in previous publication [47]. Briefly, cells were harvestedfrom cell culture and lysedwith cell lysis buffer (10mM Tris-HCl (pH7.6), 140mM NaCl, 0.5mM $CaCl_2$, 0.5mM $MgCl_2$, 0.02% NaN_3, 1% Triton X-100 and proteinase inhibitor cocktail (Sigma-Aldrich)). The protein quantification assays were performed with 2 μl cell lysate from each sample. Equal amounts of the protein extracts were loaded into wells of SDS-PAGE gel and analyzed by Western blotting. For IP, the cell lysates were precleared and mixed with the antibody conjugated to protein A/G agarose beads before incubation at 4°C with rotary agitation. The protein-antibody/beads conjugate was washed with washing buffer for 5 times to remove non-specific bindings. Any bound proteins were eluted in SDS buffer at 100°C and loaded into wells of SDS-PAGE gels for Western blotting analysis.

Chromatin immunoprecipitation (ChIP)

ChIP assays were carried out with the anti-p65 and ChIP assay kits (Millipore) according to the manufacturer's protocol. In brief, proteins and DNA were cross-linked by incubation of cells with 1%

formaldehyde. Cells were lysed and sonication was used to shear DNA to fragments of 200-1000 bp and confirmed by gel electrophoresis. The protein of interest and DNA complex were immunoprecipitated by specific antibody. The DNA fragments that were bound to the antibody were measured by PCR using primers shown in Supplementary Table S3.

Quantitative PCR (qPCR) analysis

qPCR was conducted as described in our previous publication [47]. Total RNA from cells was isolated with the ISOLATE II RNA Mini Kit (Bioline). Reverse transcription was carried out using the qScript cDNA Supermix (Quantabio). qPCR was performed at 20 µl reaction volume using SensiFAST™ SYBR Hi-ROX Kit (Bioline). All components were prepared and mixed on ice. The $2^{-\Delta\Delta CT}$ method was used to calculate the relative levels of expression of genes of interest using β-actin as endogenous control. The qPCR reaction was performed for 40 cycles: 95°C (15 s); 60°C (1 min). qPCR primers used are shown in Supplementary Table S3.

Small interference RNA and Short hairpin RNA (shRNA)

siRNAs were obtained from GenePharma (Shanghai, China). Double-stranded siRNAs were transfected in Opti-MEM medium (Invitrogen) using the Lipofectamine 2000 reagent (Invitrogen) at a final concentration of 100 nM. Medium was changed 6 hours later after transfection. The human control and ACTN4 MISSION® shRNA lentiviral transduction particles were sourced from Sigma-Aldrich (Castle Hill, NSW, Australia). Transduction of cells with virus was carried out as per the manufacturer's protocols. The medium was replaced with fresh culture medium after 24 hours. The siRNA and shRNA sequences were shown in Supplementary Table S4.

Plasmids and transfection

The lentiviral system for doxycycline-inducible gene expression (ViraPower™ HiPerform™T-REx™ Gateway® Vector Kit) was obtained from Invitrogen. The overexpression plasmid pCMV-Myc-RIPK1 was obtained from Origene. The CMX-HA-ACTN4 and GST-ACTN4 constructs were

described previously [48]. 3×Flag vector (Sigma-Aldrich) expressing ACTN4 or RIPK1 were mutated using the QuikChange Site-Directed Mutagenesis Kit (Agilent Technologies). Cells were transfected with plasmid using Lipofectamine 2000 reagent in Opti-MEM medium. The medium was replaced with fresh culture medium 6 hours later after transfection.

Melanoma xenograft mouse model

The animal experiments were conducted as our previous paper describes [45]. Approval was obtained from the Animal Research Ethics Committee of Shanxi Cancer Hospital of China. Briefly, ten male BALB/c nude mice (4-week old) were randomly assigned to two groups. Cells (1×10^7) with ACTN4 stably silenced by shRNA or control shRNA were subcutaneously injected into each flank of 4-week old male athymic nude mice (Model Animal Research Centre of Nanjing University, China). A caliper was used to assess tumor growth w every 2 days. All mice were sacrificed at the timepoint of 30 days post-transplantation. Tumours were measured and weighed.

Statistical analysis

Statistical analysis was conducted to assess differences between experimental groups using GraphPad Prism or Microsoft Excel. Specifically, two-tailed Student's *t*-test and one-way ANOVA analysis were utilised to assess differences between different groups. Statistical significance was defined as any *P*-value less than 0.05.

CONFLICT OF INTEREST

The authors declare no conflict of interest.

ACKNOWLEDGMENTS

This work was supported by the National Health and Medical Research Council (NHMRC) (APP1083496 and APP1099947) and the Natural Science Foundation of China (NSFC) (81772908). L. J. and C. C. J. are recipients of Cancer Institute NSW Fellowships.

FIGURE LEGENDS

Figure 1. ACTN4 promotes melanoma cell proliferation and melanoma xenograft growth.

a-c, shRNA silencing of ACTN4 (**a**) attenuated melanoma cell proliferation as shown in clonogenic assays (**b**) and BrdU incorporation (**c**) in Mel-CV and Mel-JD cells (n=3, mean ± S.E.M.). *P<0.05, **P<0.01, ***P<0.001, one-way ANOVA analysis. **d-f**, ACTN4 overexpression (**d**) promoted melanoma cell proliferation as shown in clonogenic assays (**e**) and BrdU incorporation (**f**) in IgR3 and Mel-RM cells (n=3, mean ± S.E.M.). *P<0.05, **P<0.01, two-tailed Student's t-test. **g-i**, ACTN4 overexpression (**g**) promoted anchorage-independent growth (**h**) and proliferation (**i**) of HEMn-MP melanocytes (n=3, mean ± S.E.M.). *P<0.05, two-tailed Student's t-test. **j-l**, silencing of ACTN4 inhibited Mel-CV xenograft growth in nu/nu mice (n=5, mean ± S.E.M.). *P<0.05, **P<0.01, two-tailed Student's t-test. **m**, silencing of ACTN4 reduced Ki67 expression in melanoma xenografts (n=5, mean immunoreactive score (IRS) ± SEM). *P<0.05, two-tailed Student's t-test. Scale bar, 100 μm.

Figure 2. ACTN4 promotes melanoma cell proliferation through NF-kB independently of its nuclear translocation.

a-d, silencing of ACTN4 in Mel-CV and Mel-JD cells diminished (**a, c**), whereas overexpression of ACTN4 in IgR3 and Mel-RM cells enhanced (**b, d**) NF-κB activity (n=3, mean ± S.E.M.). *P<0.05, **P<0.01, ***P<0.001, one-way ANOVA analysis (a) or two-tailed Student's t-test (b). **e & f**, enhancement of NF-κB activation (**e**) and melanoma cell proliferation (**f**) caused by ACTN4 overexpression was reversed by IκBα-S32AS36A in IgR3 and Mel-RM cells (n=3, mean ± S.E.M.). *P<0.05, **P<0.01, ****P<0.0001, one-way ANOVA analysis. **g**, the NF-κB inhibitors Bay-11-7082 (1 μM) and PS1145 (1 μM) diminished ACTN4 overexpression-promoted melanoma cell proliferation in IgR3 and Mel-RM cells (n=3, mean ± S.E.M.). **P<0.01, ***P<0.001, ****P<0.0001, one-way ANOVA analysis. **h & i**, inhibition of melanoma cell proliferation caused by silencing of ACTN4 was reversed by IκBα siRNA in Mel-CV and Mel-JD cells (n=3, mean ± S.E.M.). *P<0.05, one-way

ANOVA analysis. **j & k,** ACTN4 was retained in the cytoplasm of Mel-CV and Mel-JD cells under TNF-α treatment (n=3). MCF-7 cells were used as a control. Scale bar, 10 μm.

Figure 3. ACTN4 promotes activation NF-κB through RIPK1 in melanoma.

a, RIPK1 was co-precipitated with ACTN4 in Mel-CV cells (n=3). **b,** ACTN4 was co-precipitated with RIPK1 in Mel-CV cells (n=3). **c,** myc-RIPK1 purified from myc-RIPK1-overexpressing IgR3 cells was pulled down by GST-ACTN4 (n=3). **d-f,** enhancement of NF-κB activation (**e**) and melanoma cell proliferation (**f**) caused by ACTN4 overexpression (**d**) was reversed by RIPK1 siRNA in IgR3 and Mel-RM cells (*n*=3, mean ± S.E.M.). **P*<0.05, ****P*<0.001, one-way ANOVA analysis. **g-i,** inhibition of NF-κB activation (**h**) and melanoma cell proliferation (**i**) caused by silencing of ACTN4 (**g**) was reversed by inducible-overexpression of RIPK1 by Doxycycline (1 mg/mL) (*n*=3, mean ± S.E.M.). **P*<0.05, ***P*<0.01, one-way ANOVA analysis.

Figure 4. ACTN4 is critical for stabilization of RIPK1 in melanoma.

a, silencing of ACTN4 reduced RIPK1, but not cIAP1 expression in Mel-CV and Mel-JD cells (n=3). **b**, overexpression of ACTN4 increased RIPK1, but not cIAP1 expression in IgR3 and Mel-RM cells (*n*=3). **c & d**, ACTN4 silencing in Mel-CV and Mel-JD cells (**c**) or ACTN4 overexpression in IgR3 and Mel-RM cells (**d**) did not cause the alteration of RIPK1 mRNA expression levels (n=3, mean ± S.E.M.). **e**, the proteasome inhibitor MG132 (50 μM) abolished downregulation of RIPK1 caused by ACTN4 silencing (n=3). **f**, ACTN4 silencing shortened half-life time of RIPK1 protein (*n*=3, mean ± S.E.M.). **P*<0.05, ***P*<0.01, two-tailed Student's *t*-test. **g**, silencing of ACTN4 diminished K63-linked polyubiquitination of RIPK1 in Mel-CV cells (n=3). **h**, silencing of ACTN4 reduced the binding between RIPK1 and cIAP1 in Mel-CV cells (n=3).

Figure 5. ACTN4 binds to RIPK1 and cIAP1 via ABD and CLD domains respectively

a, a schematic representation of RIPK1 and the corresponding mutants. **b & c**, Flag-RIPK1-ΔDD, but not Flag-RIPK1-ΔKD and Flag-RIPK1-ΔID bound to HA-ACTN4 (**f**) or GST-ACTN4 (**g**) (n=3). **d**,

the RIPK1 kinase inhibitor Necrostatin-1 (30μM) did not impinge on the interaction between ACTN4 and RIPK1 (n=3). **e**, a schematic representation of ACTN4 and the corresponding mutants. **f**, Flag-ACTN4-ΔRD and Flag-ACTN4-ΔCLD, but not Flag-ACTN4-ΔABD bound to RIPK1 (n=3). Immunoprecipitates were subjected to Western Blotting using Flag plus ACTN4 antibodies and RIPK1 antibody. **g**, cIAP1 was co-precipitated with Flag-ACTN4 in IgR3 cells (n=3). **h,** cIAP1 purified from IgR3 cells was pulled down by GST-ACTN4 (n=3). **i**, Flag-ACTN4-ΔABD and Flag-ACTN4-ΔRD, but not Flag-ACTN4-ΔCLD bound to cIAP1 (n=3).

Figure 6. NF-κB transcriptionally activates ACTN4 in melanoma.

a, ACTN4 mRNA expression was commonly elevated in a panel of melanoma cells compared to melanocytes (*n*=3, mean ± S.E.M.). **b**, the turnover rates of ACTN4 mRNA appeared similar in cells with relatively high or low expression levels (*n*=3, mean ± S.E.M.). **c**, a schematic illustration of the human ACTN4 genomic locus. Oval: three putative p65-binding sites. **d**, a schematic illustration of pGL3-based luciferase reporter constructs containing wild-type *ACTN4* gene promoter (pGL3-ACTN4-wt) and mutant *ACTN4* gene promoter with three putative p65-binding sites deleted (pGL3-ACTN4-mut). **e**, deletion of the -984/-671 fragment abolished the transcriptional activity of *ACTN4* gene promoter (*n*=3, mean ± S.E.M.). **P*<0.05, ***P*<0.01, two-tailed Student's *t*-test. **f**, the NF-κB inhibitors BAY-11-7082 (1 μM) and PS1145 (1 μM) inhibited the transcriptional activity of *ACTN4* gene promoter (*n*=3, mean ± S.E.M.). **P*<0.05, two-tailed Student's *t*-test. **g & h**, co-transfection of IκBα siRNA diminished the transcriptional activity of *ACTN4* gene promoter (*n*=3, mean ± S.E.M.). **P*<0.05, two-tailed Student's *t*-test. **i**, NF-κB p65 subunit bound to *ACTN4* gene promoter (n=3).

REFERENCE

1. Hsu KS, Kao HY. Alpha-actinin 4 and tumorigenesis of breast cancer. Vitam Horm 2013; 93: 323-351.

2. Honda K. The biological role of actinin-4 (ACTN4) in malignant phenotypes of cancer. Cell Biosci 2015; 5: 41.

3. Honda K, Yamada T, Endo R, Ino Y, Gotoh M, Tsuda H *et al*. Actinin-4, a novel actin-bundling protein associated with cell motility and cancer invasion. J Cell Biol 1998; 140: 1383-1393.

4. Djinovic-Carugo K, Gautel M, Ylanne J, Young P. The spectrin repeat: a structural platform for cytoskeletal protein assemblies. FEBS Lett 2002; 513: 119-123.

5. Broderick MJ, Winder SJ. Towards a complete atomic structure of spectrin family proteins. J Struct Biol 2002; 137: 184-193.

6. Oikonomou KG, Zachou K, Dalekos GN. Alpha-actinin: a multidisciplinary protein with important role in B-cell driven autoimmunity. Autoimmun Rev 2011; 10: 389-396.

7. Kakuya T, Mori T, Yoshimoto S, Watabe Y, Miura N, Shoji H *et al*. Prognostic significance of gene amplification of ACTN4 in stage I and II oral tongue cancer. Int J Oral Maxillofac Surg 2017.

8. Watanabe T, Ueno H, Watabe Y, Hiraoka N, Morizane C, Itami J *et al*. ACTN4 copy number increase as a predictive biomarker for chemoradiotherapy of locally advanced pancreatic cancer. Br J Cancer 2015; 112: 704-713.

9. Yamamoto S, Tsuda H, Honda K, Onozato K, Takano M, Tamai S *et al*. Actinin-4 gene amplification in ovarian cancer: a candidate oncogene associated with poor patient prognosis and tumor chemoresistance. Mod Pathol 2009; 22: 499-507.

10. Noro R, Honda K, Tsuta K, Ishii G, Maeshima AM, Miura N *et al*. Distinct outcome of stage I lung adenocarcinoma with ACTN4 cell motility gene amplification. Ann Oncol 2013; 24: 2594-2600.

11. Watabe Y, Mori T, Yoshimoto S, Nomura T, Shibahara T, Yamada T *et al*. Copy number increase of ACTN4 is a prognostic indicator in salivary gland carcinoma. Cancer Med 2014; 3: 613-622.

12. Yamamoto S, Tsuda H, Honda K, Takano M, Tamai S, Imoto I *et al*. ACTN4 gene amplification and actinin-4 protein overexpression drive tumour development and histological progression in a high-grade subset of ovarian clear-cell adenocarcinomas. Histopathology 2012; 60: 1073-1083.

13. Gao Y, Li G, Sun L, He Y, Li X, Sun Z *et al*. ACTN4 and the pathways associated with cell motility and adhesion contribute to the process of lung cancer metastasis to the brain. BMC Cancer 2015; 15: 277.

14. Shao H, Li S, Watkins SC, Wells A. alpha-Actinin-4 is required for amoeboid-type invasiveness of melanoma cells. J Biol Chem 2014; 289: 32717-32728.

15. Aksenova V, Turoverova L, Khotin M, Magnusson KE, Tulchinsky E, Melino G *et al*. Actin-binding protein alpha-actinin 4 (ACTN4) is a transcriptional co-activator of RelA/p65 sub-unit of NF-kB. Oncotarget 2013; 4: 362-372.

16. Khurana S, Chakraborty S, Cheng X, Su YT, Kao HY. The actin-binding protein, actinin alpha 4 (ACTN4), is a nuclear receptor coactivator that promotes proliferation of MCF-7 breast cancer cells. J Biol Chem 2011; 286: 1850-1859.

17. Agarwal N, Adhikari AS, Iyer SV, Hekmatdoost K, Welch DR, Iwakuma T. MTBP suppresses cell migration and filopodia formation by inhibiting ACTN4. Oncogene 2013; 32: 462-470.

18. Babakov VN, Petukhova OA, Turoverova LV, Kropacheva IV, Tentler DG, Bolshakova AV *et al*. RelA/NF-kappaB transcription factor associates with alpha-actinin-4. Exp Cell Res 2008; 314: 1030-1038.

19. Ding Z, Liang J, Lu Y, Yu Q, Songyang Z, Lin SY *et al*. A retrovirus-based protein complementation assay screen reveals functional AKT1-binding partners. Proc Natl Acad Sci U S A 2006; 103: 15014-15019.

20. Carragher NO, Fincham VJ, Riley D, Frame MC. Cleavage of focal adhesion kinase by different proteases during SRC-regulated transformation and apoptosis. Distinct roles for calpain and caspases. J Biol Chem 2001; 276: 4270-4275.

21. Sjoblom B, Salmazo A, Djinovic-Carugo K. Alpha-actinin structure and regulation. Cell Mol Life Sci 2008; 65: 2688-2701.

22. Shao H, Wu C, Wells A. Phosphorylation of alpha-actinin 4 upon epidermal growth factor exposure regulates its interaction with actin. J Biol Chem 2010; 285: 2591-2600.

23. Festjens N, Vanden Berghe T, Cornelis S, Vandenabeele P. RIP1, a kinase on the crossroads of a cell's decision to live or die. Cell Death Differ 2007; 14: 400-410.

24. Wang L, Du F, Wang X. TNF-alpha induces two distinct caspase-8 activation pathways. Cell 2008; 133: 693-703.

25. Christofferson DE, Li Y, Hitomi J, Zhou W, Upperman C, Zhu H *et al*. A novel role for RIP1 kinase in mediating TNFalpha production. Cell Death Dis 2012; 3: e320.

26. Liu XY, Lai F, Yan XG, Jiang CC, Guo ST, Wang CY *et al*. RIP1 Kinase Is an Oncogenic Driver in Melanoma. Cancer Res 2015; 75: 1736-1748.

27. Luan Q, Jin L, Jiang CC, Tay KH, Lai F, Liu XY *et al*. RIPK1 regulates survival of human melanoma cells upon endoplasmic reticulum stress through autophagy. Autophagy 2015; 11: 975-994.

28. Jin L, Chen J, Liu XY, Jiang CC, Zhang XD. The double life of RIPK1. Mol Cell Oncol 2016; 3: e1035690.

29. Ofengeim D, Yuan J. Regulation of RIP1 kinase signalling at the crossroads of inflammation and cell death. Nat Rev Mol Cell Biol 2013; 14: 727-736.

30. Bertrand MJ, Milutinovic S, Dickson KM, Ho WC, Boudreault A, Durkin J *et al*. cIAP1 and cIAP2 facilitate cancer cell survival by functioning as E3 ligases that promote RIP1 ubiquitination. Mol Cell 2008; 30: 689-700.

31. Blackwell K, Zhang L, Workman LM, Ting AT, Iwai K, Habelhah H. Two coordinated mechanisms underlie tumor necrosis factor alpha-induced immediate and delayed IkappaB kinase activation. Mol Cell Biol 2013; 33: 1901-1915.

32. Moquin DM, McQuade T, Chan FK. CYLD deubiquitinates RIP1 in the TNFalpha-induced necrosome to facilitate kinase activation and programmed necrosis. PLoS One 2013; 8: e76841.

33. Karin M. How NF-kappaB is activated: the role of the IkappaB kinase (IKK) complex. Oncogene 1999; 18: 6867-6874.

34. Vince JE, Wong WW, Khan N, Feltham R, Chau D, Ahmed AU *et al*. IAP antagonists target cIAP1 to induce TNFalpha-dependent apoptosis. Cell 2007; 131: 682-693.

35. Cerami E, Gao J, Dogrusoz U, Gross BE, Sumer SO, Aksoy BA *et al*. The cBio cancer genomics portal: an open platform for exploring multidimensional cancer genomics data. Cancer Discov 2012; 2: 401-404.

36. Gao J, Aksoy BA, Dogrusoz U, Dresdner G, Gross B, Sumer SO *et al*. Integrative analysis of complex cancer genomics and clinical profiles using the cBioPortal. Sci Signal 2013; 6: pl1.

37. Dong L, Jin L, Tseng HY, Wang CY, Wilmott JS, Yosufi B *et al*. Oncogenic suppression of PHLPP1 in human melanoma. Oncogene 2014; 33: 4756-4766.

38. Babakov VN, Bobkov DE, Petukhova OA, Turoverova LV, Kropacheva IV, Podol'skaia EP *et al*. [alpha-Actinin-4 and p65/RelA subunit of NF-kappaB transcription factor are co-localized and migrate together into the nucleus in EGF-stimulated A431 cell]. Tsitologiia 2004; 46: 1064-1072.

39. Kumeta M, Yoshimura SH, Harata M, Takeyasu K. Molecular mechanisms underlying nucleocytoplasmic shuttling of actinin-4. J Cell Sci 2010; 123: 1020-1030.

40. Fagerlund R, Kinnunen L, Kohler M, Julkunen I, Melen K. NF-{kappa}B is transported into the nucleus by importin {alpha}3 and importin {alpha}4. J Biol Chem 2005; 280: 15942-15951.

41. Shao H, Travers T, Camacho CJ, Wells A. The carboxyl tail of alpha-actinin-4 regulates its susceptibility to m-calpain and thus functions in cell migration and spreading. Int J Biochem Cell Biol 2013; 45: 1051-1063.

42. Karin M, Lin A. NF-kappaB at the crossroads of life and death. Nat Immunol 2002; 3: 221-227.

43. Jin L, Hu WL, Jiang CC, Wang JX, Han CC, Chu P *et al*. MicroRNA-149*, a p53-responsive microRNA, functions as an oncogenic regulator in human melanoma. Proc Natl Acad Sci U S A 2011; 108: 15840-15845.

44. Dong L, Jiang CC, Thorne RF, Croft A, Yang F, Liu H *et al*. Ets-1 mediates upregulation of Mcl-1 downstream of XBP-1 in human melanoma cells upon ER stress. Oncogene 2011; 30: 3716-3726.

45. Ye Y, Jin L, Wilmott JS, Hu WL, Yosufi B, Thorne RF *et al*. PI(4,5)P2 5-phosphatase A regulates PI3K/Akt signalling and has a tumour suppressive role in human melanoma. Nat Commun 2013; 4: 1508.

46. Hu W, Jin L, Jiang CC, Long GV, Scolyer RA, Wu Q *et al*. AEBP1 upregulation confers acquired resistance to BRAF (V600E) inhibition in melanoma. Cell Death Dis 2013; 4: e914.

47. Tay KH, Jin L, Tseng HY, Jiang CC, Ye Y, Thorne RF *et al*. Suppression of PP2A is critical for protection of melanoma cells upon endoplasmic reticulum stress. Cell Death Dis 2012; 3: e337.

48. Zhao X, Hsu KS, Lim JH, Bruggeman LA, Kao HY. alpha-Actinin 4 potentiates nuclear factor kappa-light-chain-enhancer of activated B-cell (NF-kappaB) activity in podocytes independent of its cytoplasmic actin binding function. J Biol Chem 2015; 290: 338-349.

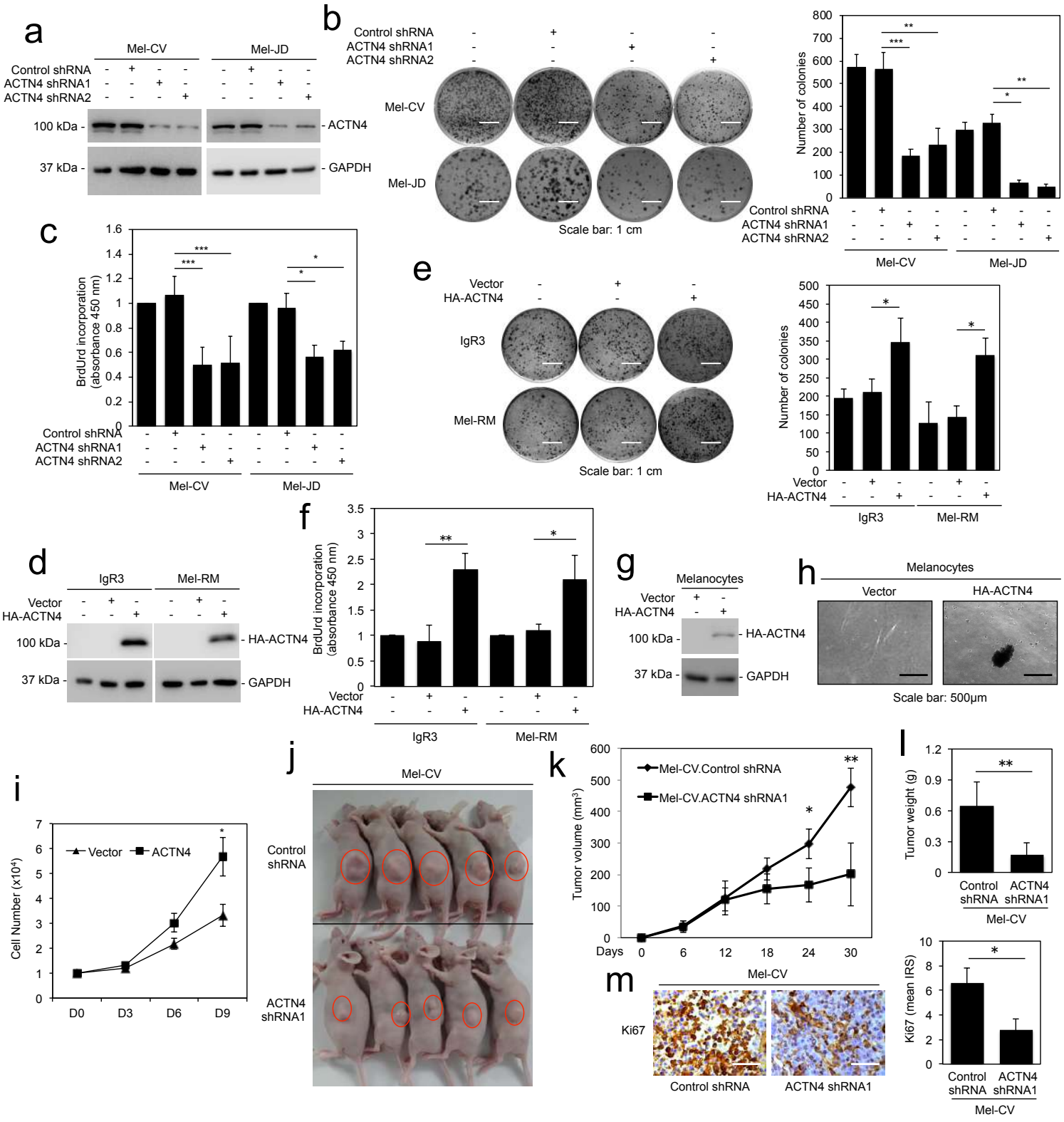
a
Mel-CV
Mel-JD
Control shRNA
ACTN4 shRNA1
ACTN4 shRNA2
100 kDa
ACTN4
37 kDa
GAPDH
b
Control shRNA
ACTN4 shRNA1
ACTN4 shRNA2
Mel-CV
Mel-JD
Scale bar: 1 cm
Number of colonies
c
BrdUrd incorporation (absorbance 450 nm)
e
Vector
HA-ACTN4
IgR3
Mel-RM
Scale bar: 1 cm
Number of colonies
d
IgR3
Mel-RM
Vector
HA-ACTN4
100 kDa
HA-ACTN4
37 kDa
GAPDH
f
BrdUrd incorporation (absorbance 450 nm)
g
Melanocytes
Vector
HA-ACTN4
100 kDa
HA-ACTN4
37 kDa
GAPDH
h
Melanocytes
Vector
HA-ACTN4
Scale bar: 500μm
i
Cell Number (x10⁴)
Vector
ACTN4
D0
D3
D6
D9
j
Mel-CV
Control shRNA
ACTN4 shRNA1
k
Mel-CV.Control shRNA
Mel-CV.ACTN4 shRNA1
Tumor volume (mm³)
Days
l
Tumor weight (g)
Control shRNA
ACTN4 shRNA1
Mel-CV
m
Mel-CV
Ki67
Control shRNA
ACTN4 shRNA1
Ki67 (mean IRS)

Figure 1

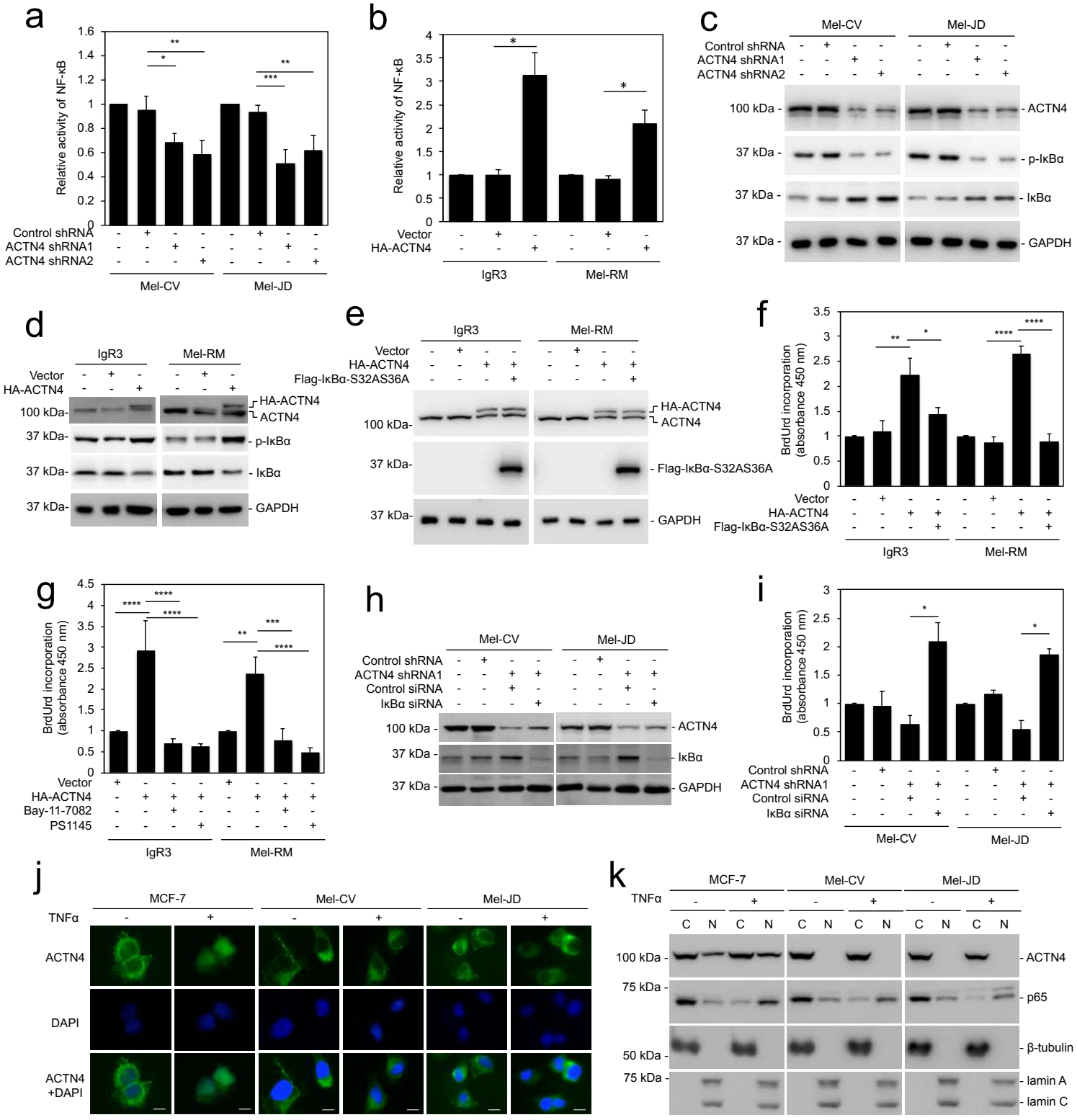
a
Relative activity of NF-κB
Control shRNA
ACTN4 shRNA1
ACTN4 shRNA2
Mel-CV
Mel-JD
b
Relative activity of NF-κB
Vector
HA-ACTN4
IgR3
Mel-RM
c
Mel-CV
Mel-JD
Control shRNA
ACTN4 shRNA1
ACTN4 shRNA2
100 kDa
37 kDa
ACTN4
p-IκBα
IκBα
GAPDH
d
IgR3
Mel-RM
Vector
HA-ACTN4
100 kDa
37 kDa
HA-ACTN4
ACTN4
p-IκBα
IκBα
GAPDH
e
IgR3
Mel-RM
Vector
HA-ACTN4
Flag-IκBα-S32AS36A
100 kDa
37 kDa
HA-ACTN4
ACTN4
Flag-IκBα-S32AS36A
GAPDH
f
BrdUrd incorporation (absorbance 450 nm)
Vector
HA-ACTN4
Flag-IκBα-S32AS36A
IgR3
Mel-RM
g
BrdUrd incorporation (absorbance 450 nm)
Vector
HA-ACTN4
Bay-11-7082
PS1145
IgR3
Mel-RM
h
Mel-CV
Mel-JD
Control shRNA
ACTN4 shRNA1
Control siRNA
IκBα siRNA
100 kDa
37 kDa
37 kDa
ACTN4
IκBα
GAPDH
i
BrdUrd incorporation (absorbance 450 nm)
Control shRNA
ACTN4 shRNA1
Control siRNA
IκBα siRNA
Mel-CV
Mel-JD
j
MCF-7
Mel-CV
Mel-JD
TNFα
ACTN4
DAPI
ACTN4 +DAPI
k
MCF-7
Mel-CV
Mel-JD
TNFα
C N C N C N C N C N C N
100 kDa
75 kDa
50 kDa
75 kDa
ACTN4
p65
β-tubulin
lamin A
lamin C

Figure 2

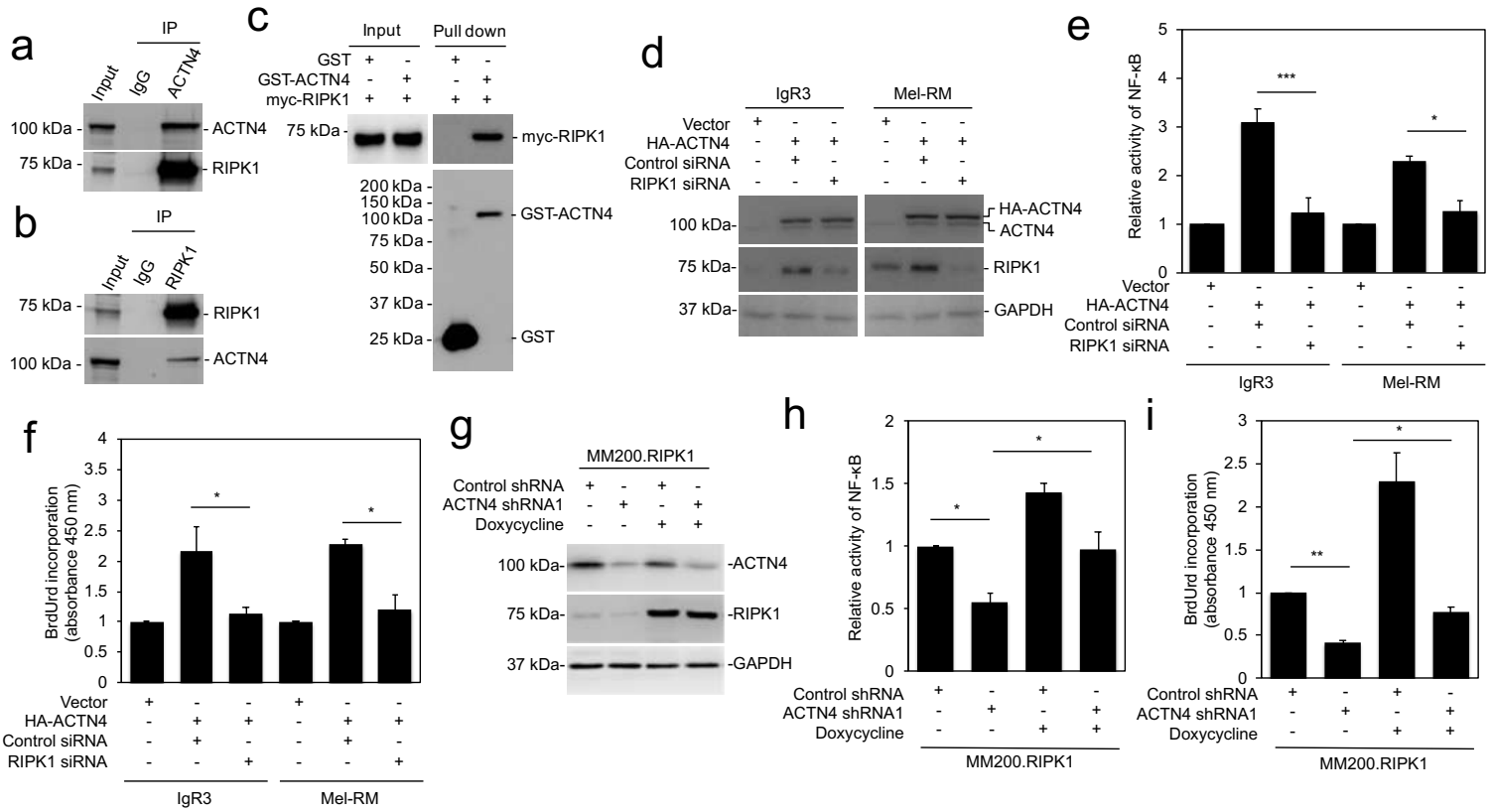
a
IP
Input
IgG
ACTN4
100 kDa
75 kDa
ACTN4
RIPK1
b
IP
Input
IgG
RIPK1
75 kDa
100 kDa
RIPK1
ACTN4
c
Input
Pull down
GST
GST-ACTN4
myc-RIPK1
75 kDa
200 kDa
150 kDa
100 kDa
75 kDa
50 kDa
37 kDa
25 kDa
myc-RIPK1
GST-ACTN4
GST
d
IgR3
Mel-RM
Vector
HA-ACTN4
Control siRNA
RIPK1 siRNA
100 kDa
75 kDa
37 kDa
HA-ACTN4
ACTN4
RIPK1
GAPDH
e
Relative activity of NF-κB
***
*
Vector
HA-ACTN4
Control siRNA
RIPK1 siRNA
IgR3
Mel-RM
f
BrdUrd incorporation (absorbance 450 nm)
*
*
Vector
HA-ACTN4
Control siRNA
RIPK1 siRNA
IgR3
Mel-RM
g
MM200.RIPK1
Control shRNA
ACTN4 shRNA1
Doxycycline
100 kDa
75 kDa
37 kDa
ACTN4
RIPK1
GAPDH
h
Relative activity of NF-κB
*
*
Control shRNA
ACTN4 shRNA1
Doxycycline
MM200.RIPK1
i
BrdUrd incorporation (absorbance 450 nm)
**
*
Control shRNA
ACTN4 shRNA1
Doxycycline
MM200.RIPK1

Figure 3

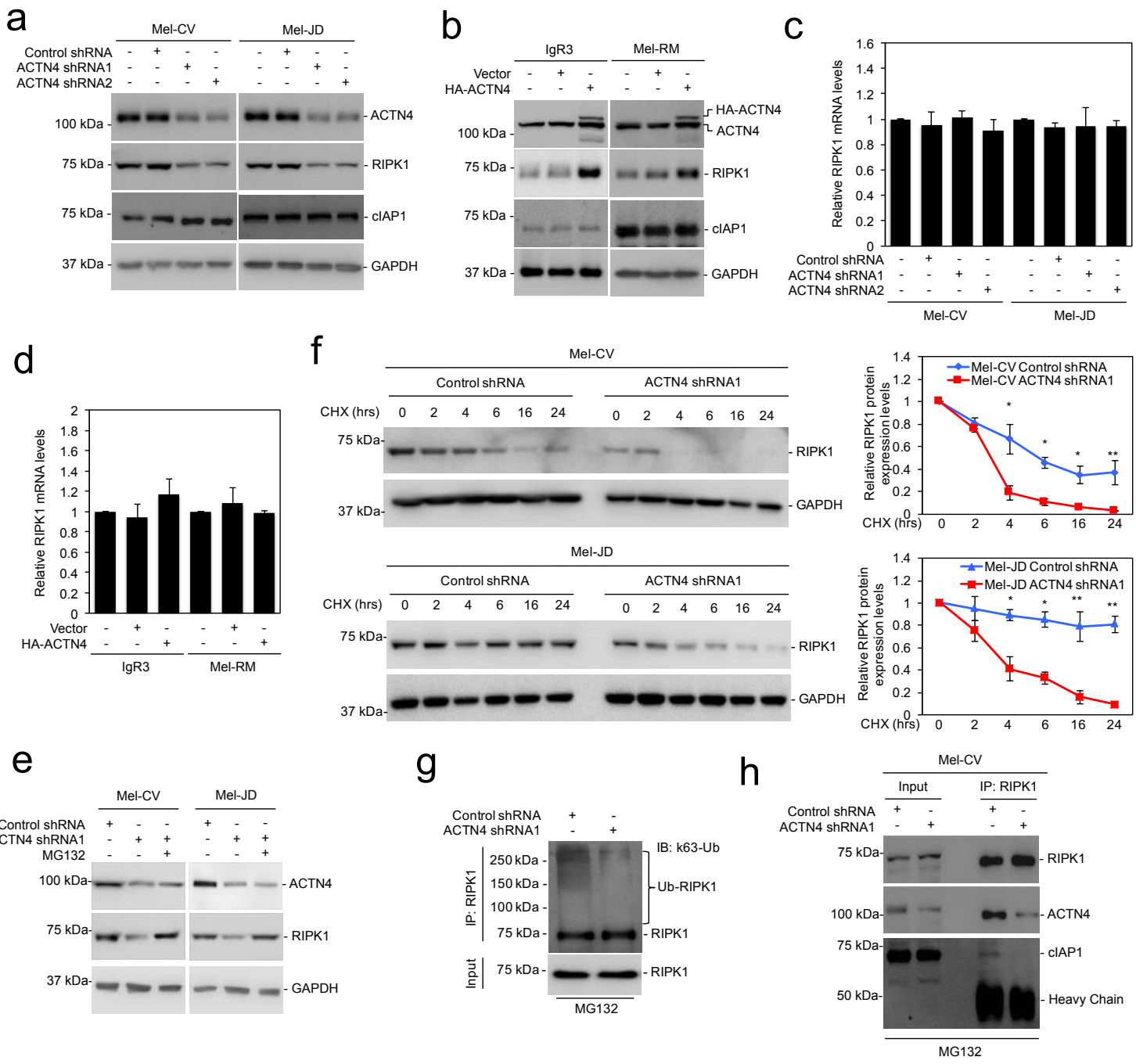
a
Mel-CV
Mel-JD
Control shRNA
ACTN4 shRNA1
ACTN4 shRNA2
100 kDa
75 kDa
75 kDa
37 kDa
ACTN4
RIPK1
cIAP1
GAPDH
b
IgR3
Mel-RM
Vector
HA-ACTN4
100 kDa
75 kDa
75 kDa
37 kDa
HA-ACTN4
ACTN4
RIPK1
cIAP1
GAPDH
c
Relative RIPK1 mRNA levels
Control shRNA
ACTN4 shRNA1
ACTN4 shRNA2
Mel-CV
Mel-JD
d
Relative RIPK1 mRNA levels
Vector
HA-ACTN4
IgR3
Mel-RM
f
Mel-CV
Control shRNA
ACTN4 shRNA1
CHX (hrs)
0 2 4 6 16 24
75 kDa
37 kDa
RIPK1
GAPDH
Mel-JD
Relative RIPK1 protein expression levels
Mel-CV Control shRNA
Mel-CV ACTN4 shRNA1
Mel-JD Control shRNA
Mel-JD ACTN4 shRNA1
e
Mel-CV
Mel-JD
Control shRNA
ACTN4 shRNA1
MG132
100 kDa
75 kDa
37 kDa
ACTN4
RIPK1
GAPDH
g
Control shRNA
ACTN4 shRNA1
IP: RIPK1
250 kDa
150 kDa
100 kDa
75 kDa
Input
75 kDa
IB: k63-Ub
Ub-RIPK1
RIPK1
RIPK1
MG132
h
Mel-CV
Input
IP: RIPK1
Control shRNA
ACTN4 shRNA1
75 kDa
100 kDa
75 kDa
50 kDa
RIPK1
ACTN4
cIAP1
Heavy Chain
MG132

Figure 4

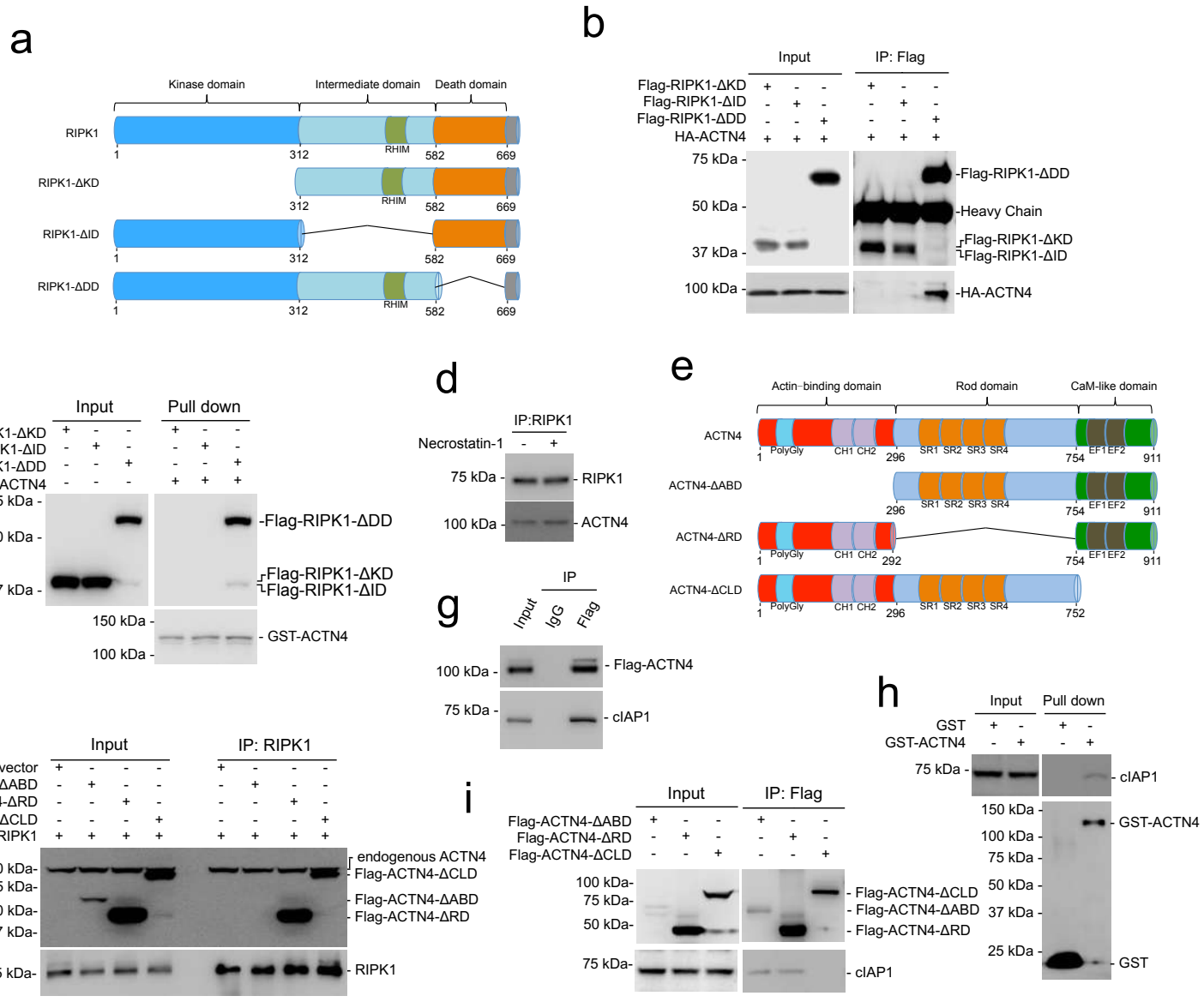
a
Kinase domain
Intermediate domain
Death domain
RIPK1
RIPK1-ΔKD
RIPK1-ΔID
RIPK1-ΔDD
RHIM
1
312
582
669
b
Input
IP: Flag
Flag-RIPK1-ΔKD
Flag-RIPK1-ΔID
Flag-RIPK1-ΔDD
HA-ACTN4
75 kDa
50 kDa
37 kDa
100 kDa
-Flag-RIPK1-ΔDD
-Heavy Chain
-Flag-RIPK1-ΔKD
-Flag-RIPK1-ΔID
-HA-ACTN4
c
Input
Pull down
Flag-RIPK1-ΔKD
Flag-RIPK1-ΔID
Flag-RIPK1-ΔDD
GST-ACTN4
75 kDa
50 kDa
37 kDa
150 kDa
100 kDa
-Flag-RIPK1-ΔDD
-Flag-RIPK1-ΔKD
-Flag-RIPK1-ΔID
- GST-ACTN4
d
IP:RIPK1
Necrostatin-1
75 kDa
100 kDa
- RIPK1
- ACTN4
e
Actin-binding domain
Rod domain
CaM-like domain
ACTN4
ACTN4-ΔABD
ACTN4-ΔRD
ACTN4-ΔCLD
PolyGly
CH1 CH2
SR1 SR2 SR3 SR4
EF1 EF2
1
296
754
911
292
752
f
Input
IP: RIPK1
Flag-vector
Flag-ACTN4-ΔABD
Flag-ACTN4-ΔRD
Flag-ACTN4-ΔCLD
myc-RIPK1
100 kDa-
75 kDa-
50 kDa-
37 kDa-
endogenous ACTN4
Flag-ACTN4-ΔCLD
Flag-ACTN4-ΔABD
Flag-ACTN4-ΔRD
- RIPK1
g
IP
Input
IgG
Flag
100 kDa -
75 kDa -
- Flag-ACTN4
- cIAP1
h
Input
Pull down
GST
GST-ACTN4
75 kDa -
150 kDa -
100 kDa -
50 kDa -
37 kDa -
25 kDa -
- cIAP1
- GST-ACTN4
- GST
i
Input
IP: Flag
Flag-ACTN4-ΔABD
Flag-ACTN4-ΔRD
Flag-ACTN4-ΔCLD
100 kDa-
75 kDa-
50 kDa-
- Flag-ACTN4-ΔCLD
- Flag-ACTN4-ΔABD
- Flag-ACTN4-ΔRD
- cIAP1

Figure 5

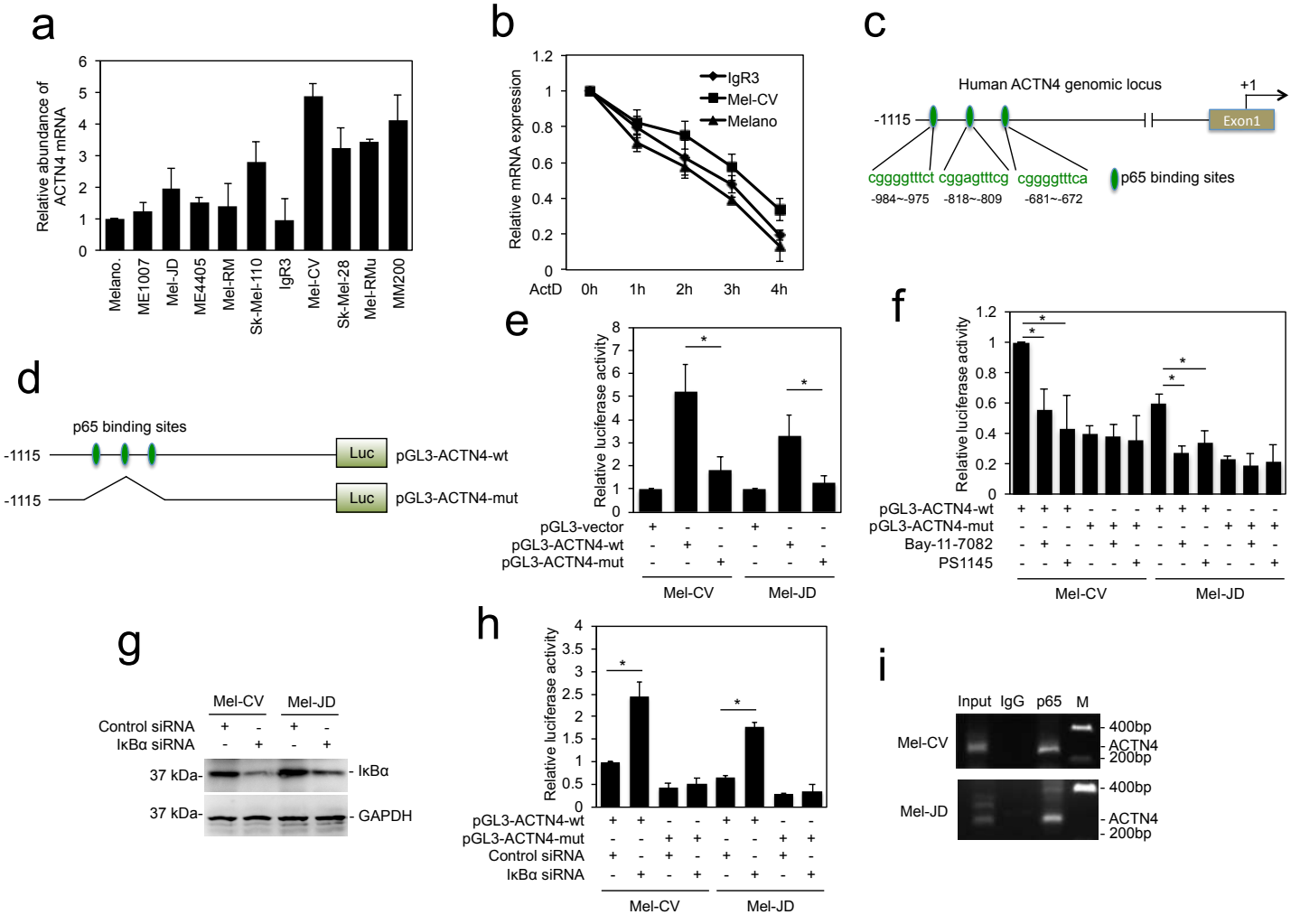
a
Relative abundance of ACTN4 mRNA
Melano.
ME1007
Mel-JD
ME4405
Mel-RM
Sk-Mel-110
IgR3
Mel-CV
Sk-Mel-28
Mel-RMu
MM200
b
Relative mRNA expression
IgR3
Mel-CV
Melano
ActD 0h 1h 2h 3h 4h
c
Human ACTN4 genomic locus
+1
-1115
Exon1
cggggtttct
cggagtttcg
cgggggtttca
p65 binding sites
-984~-975
-818~-809
-681~-672
d
p65 binding sites
-1115
Luc
pGL3-ACTN4-wt
-1115
Luc
pGL3-ACTN4-mut
e
Relative luciferase activity
pGL3-vector
pGL3-ACTN4-wt
pGL3-ACTN4-mut
Mel-CV
Mel-JD
f
Relative luciferase activity
pGL3-ACTN4-wt
pGL3-ACTN4-mut
Bay-11-7082
PS1145
Mel-CV
Mel-JD
g
Mel-CV
Mel-JD
Control siRNA
IκBα siRNA
37 kDa-
- IκBα
37 kDa-
- GAPDH
h
Relative luciferase activity
pGL3-ACTN4-wt
pGL3-ACTN4-mut
Control siRNA
IκBα siRNA
Mel-CV
Mel-JD
i
Input IgG p65 M
Mel-CV
Mel-JD
- 400bp
- ACTN4
- 200bp
- 400bp
- ACTN4
- 200bp

Figure 6